FERMILAB-CONF-22-834-V
20th Int. Conf. on RF Superconductivity SRF2021, East Lansing, MI, USA JACoW Publishing
ISBN: 978-3-95450-233-2 ISSN: 2673-5504 doi:10.18429/JACoW-SRF2021-TUPFDV007

SURFACE IMPEDANCE OF Nb_3Sn AND $YBa_2Cu_3O_{7-\delta}$ IN HIGH MAGNETIC FIELDS

N. Pompeo*, A. Alimenti, K. Torokhtii, E. Silva, Engineering Dep., Università Roma Tre, Roma, Italy
G. Celentano, V. Pinto, F. Rizzo, ENEA Frascati, Roma, Italy
T. Spina, Fermilab, Batavia, Illinois, USA
R. Flükiger, Geneva University, Geneva, Switzerland

Abstract

New potential rf applications of superconductors are emerging with the need to operate in high dc magnetic fields (up to 16 T) where vortex motion dictates the response: the beam screen coating of the Future Circular Collider (FCC) and haloscopes, i.e. rf cavities for the axions detection. We present in this work measurements of the surface impedance Z_s up to 12 T on bulk Nb_3Sn and $YBa_2Cu_3O_{7-\delta}$ thin films by means of a dielectric loaded resonator operating at 15 GHz. We obtained the vortex motion resistivity and extracted the depinning frequency, the flux-flow resistivity and the pinning constant. Substantial differences are highlighted in the high frequency pinning properties of the studied materials, providing useful information on possible improvements in view of applications.

INTRODUCTION

Particle accelerators have for a long time benefited by the application of superconducting materials at radio frequency (rf) in zero static magnetic fields, allowing for resonant cavities with very high quality factors Q and thus providing very intense accelerating electric fields. Recently, a new field for the application of superconductors (SC) at microwave and radio frequencies opened up, namely the search for low surface resistance in high or very high dc magnetic fields. Examples are the beam screen in the Future Circular Collider project at CERN (frequencies up to f ~1.5 GHz [1], in static magnetic fields up to B =16 T at temperature $T = 50$ K), and haloscopes in dark matter research (high Q cavities operating in static magnetic B of the order of a few tesla [2]).

In the foreseen operating conditions the main source of losses in the superconductor arises from the dissipative motion of quantized magnetic flux lines (called fluxons or vortices) under the action of the alternating currents, making the zero-field surface resistance completely irrelevant. Minimization of these losses involves the reduction of fluxon motion by introducing suitable defects (vortex pinning centers). Engineered pinning centers in $YBa_2Cu_3O_{7-\delta}$ (YBCO) were found to strongly improve the performances in d.c. [3,4]. Moreover, it was shown long since [5] that the same nano-engineered defects are effective in reducing the microwave surface resistance $R_s := \mathrm{Re}(Z_s)$ of YBCO in moderate fields ($B \lesssim 1$ T), by increasing the pinning efficiency (measured by the so-called pinning constant k_p) also in the high frequency dynamics regime, although through a different pinning mechanism [6]. This effect was also observed in YBCO coated conductors (CC) [7,8], and regardless of the pristine material anisotropy [9]. Very recently, studies up to 9 T [10] in YBCO CC and up to 12 T [11] in YBCO thin films showed the effectiveness of artificial pinning centers (APC) at high fields, too.

With respect to the studies in YBCO, very little is known about the rf behaviour in the mixed state of Nb_3Sn, the workhorse of superconducting materials, promising as a successor of Nb in rf accelerating cavities [12], in moderate static magnetic fields.

Aim of this work is to present and compare sample studies on Nb_3Sn and YBCO. We report on microwave measurements at high magnetic fields ($\mu_0 H \leq 12$ T) of the surface impedance Z_s, and extract the relevant fluxon parameters through the established model for vortex motion, which is discussed in the following.

MODEL AND METHODS

The high frequency complex resistivity $\tilde{\rho}$ in the mixed state in the linear regime is [13]

$$\tilde{\rho} = \frac{\rho_{vm} + \mathrm{i}/\sigma_2}{1 + \mathrm{i}\sigma_1/\sigma_2} \quad (1)$$

where $\sigma = \sigma_1 - \mathrm{i}\sigma_2$ is the two fluid conductivity and ρ_{vm} is the vortex motion resistivity. The vortex motion resistivity depends on three physical mechanisms: the free motion of vortices, leading to dissipation in the vortex core, the vortex pinning, leading to elastic recall of the vortex with pinning constant k_p, and finally the thermally activated jumps from one pinning site to another, called flux creep. These mechanisms are built in the following expression:

$$\rho_{vm} = \rho_{vm,1} + \mathrm{i}\rho_{vm,2} = \rho_{ff}\frac{\chi + \mathrm{i}\nu/\nu_c}{1 + \mathrm{i}\nu/\nu_c} \quad (2)$$

where $\rho_{ff} = \Phi_0 B/\eta$ is the free-flux flow resistivity (as in absence of pinning), η is the so-called vortex viscosity, $\chi \in [0,1]$ is an adimensional creep factor (where $\chi = 0$ means no creep and $\chi = 1$ denotes maximum creep, condition in which creep completely washes out the pinning potential yielding $\rho_{vm} = \rho_{ff}$). The characteristic frequency ν_c is a combination of the creep factor and of the pinning frequency $\nu_p = k_p/(\eta 2\pi)$, and it is $\nu_c(\chi = 0) = \nu_p$ (the $\chi = 0$ model has been worked out longtime ago [14]). ν_c represents a synthetic evaluation of the (relative) amount of losses, as depicted in the plot of $\rho_{vm}(\nu)$ in Fig. 1.

* nicola.pompeo@uniroma3.it

This manuscript has been authored by Fermi Research Alliance, LLC under Contract No. DE-AC02-07CH11359 with the U.S. Department of Energy, Office of Science, Office of High Energy Physics.

ISBN: 978-3-95450-233-2 ISSN: 2673-5504 doi:10.18429/JACoW-SRF2021-TUPFDV007

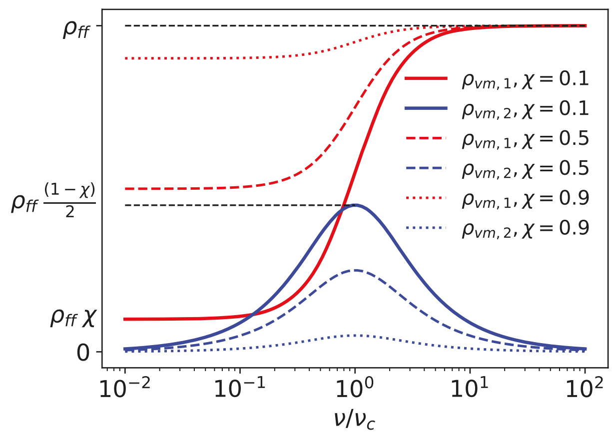

Figure 1: Frequency dependence of the real and imaginary parts of ρ_{vm}, Eq. (2), plotted for $\chi = \{0.1, 0.5, 0.9\}$.

The SC resistivity at microwaves is related to the measured surface impedance Z_s by geometry-dependent relations. For the present purposes, one is concerned with electromagnetically thick samples (sample thickness $d \gg \max(\delta, \lambda)$, where δ and λ are the skin penetration depth and London length, respectively), where:

$$Z_s = \sqrt{i2\pi\nu\mu_0\tilde{\rho}} \simeq \sqrt{i2\pi\nu\mu_0\left(\rho_{vm} + \mathrm{i}\frac{1}{\sigma_2}\right)} \qquad (3)$$

where the last approximation holds for $T \lesssim 0.95T_c(H)$, and electromagnetically thin samples, where:

$$Z_s \simeq \frac{\tilde{\rho}}{d} \qquad (4)$$

The surface impedance $Z_s = R_s + \mathrm{i}X_s$ is here measured by means of a dielectric loaded resonator (DR) within a perturbation approach, where the sample under study replaces one of the DR end-walls. For a selected resonant mode, the (unloaded) quality factor Q and the shift of the resonant frequency ν_r with the applied magnetic field H, at fixed T, are related to the field induced variations $\Delta Z_s(H) = Z_s(H) - Z_s(0)$, relevant for vortex dynamics studies, as follows [15]:

$$\Delta Z_s(H) = G\left[\left(\frac{1}{Q(H)} - \frac{1}{Q(0)}\right) - 2\mathrm{i}\frac{\nu_r(H) - \nu_r(0)}{\nu_r(0)}\right] \qquad (5)$$

where G is a geometric factor, numerically computed, related to the end-wall surface portion covered by the sample.

As described in [15], the samples are placed on a base of a cylindrical DR, loaded with a coaxial sapphire cylinder with diameter 8.00 mm and height 5.00 mm, operated in the transverse-electric TE_{011} mode at $\nu_r \simeq 14.9$ GHz. The resonator is placed in a He-flow cryomagnet, producing up to 12 T. The resonator parameters Q and ν_r are determined by measuring, with a Vector Network Analyser, the frequency dependent two-port scattering coefficients $S_{ij}(\nu)$ of the DR operated in transmission and by fitting them with models for its resonant response. Additional effects due to various non-idealities (microwave line partial calibration, cross coupling between the resonator ports) are specifically taken into account with extended models [16].

RESULTS AND DISCUSSION

We measured Z in a platelet of Nb_3Sn and in a thin YBCO film grown from a solution at 5% mol. $BaZrO_3$ (Table 1), which produces nanosize second phases of $BaZrO_3$ that act as strong pinning centers [17].

Table 1: Samples

	Nb_3Sn	YBCO
T_c	17.9 K	89.7 K
shape	bulk platelet	thin film
size	area 30 mm^2	7.5×7.5 mm^2, d=100 nm
substrate	-	$SrTiO_3$
growth	Hot Isostatic Pressure [18]	Chemical Solution Deposition [17]

Typical measurements of $\Delta Z_s(H)$ are reported in Figure 2 at temperatures chosen to yield the same reduced temperature values $T/T_c \simeq 0.3$. The common increasing trend

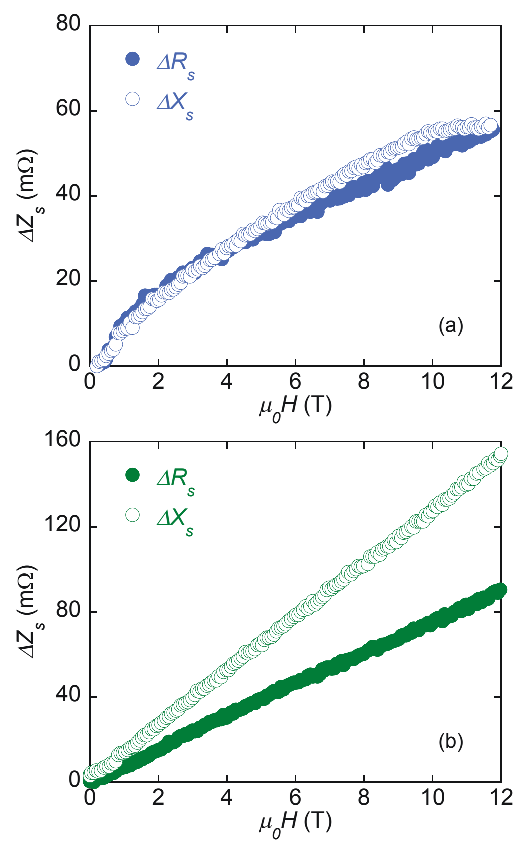

Figure 2: $\Delta Z_s(H)$ vs field H in Nb_3Sn [19] (panel (a), T = 6.0 K) and YBCO (panel (b), T = 27.0 K). Temperatures are selected in order to yield the same $T/T_c \simeq 0.3$.

with B, basically due to the increase of fluxon number $\propto B$ in

ISBN: 978-3-95450-233-2 ISSN: 2673-5504 doi:10.18429/JACoW-SRF2021-TUPFDV007

the superconductors, takes different functional dependences according to the different geometries (Eqs. (3),(4)) [20]: approximately $\propto \sqrt{B}$ in the bulk Nb_3Sn and $\propto B$ in YBCO thin film. The highlighted functional depedences point to a field dependent dominant contribution given by $\rho_{ff} \propto B$ (see Eq.(2)), suggesting that the fluxon parameters exhibit little B-dependences. We note that a direct comparison of the absolute values of e.g. R_s is of little physical significance, due to the different sample thicknesses (bulk vs. film). A more meaningful comparison involves the vortex motion resistivity which is extracted as follows:

- for Nb_3Sn, Eq. (5) is inverted to explicit ρ_{vm}, taking $\sigma_2 = 1/(2\pi\nu\mu_0\lambda)$ with $\lambda = 130$ nm (details in [19]);
- for YBCO, $\rho_{vm}(H) = \Delta Z_s(H)d$, from Eq.(4).

Figure 3 reports a comparison of ρ_{vm} at $T/T_c \simeq 0.3$ in Nb_3Sn and YBCO. From the comparison of $\rho_{vm,1}$, it can be seen

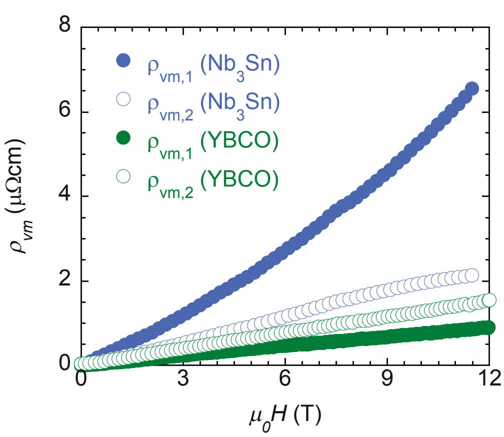

Figure 3: ρ_{vm} vs H as extracted from the data for Z_s in Fig.2 for Nb_3Sn and YBCO at the same $T/T_c \simeq 0.3$.

that YBCO exhibits lower dissipation. One also notes that $\rho_{vm,2} > \rho_{vm,1}$ in YBCO (with respect to) the contrary in Nb_3Sn). In view of Eq. (2), this fact points to higher pinning in YBCO. A quantitative analysis comes from the evaluation of the fluxon parameters. From ρ_{vm}, and assuming negligible creep (i.e. assuming $\chi = 0$; the error bars originating from this assumption have been extensively discussed in [21]), the vortex viscosity η and the pinning frequency ν_p (whence k_p) can be extracted. The analysis of the data assuming $\chi = 0$ in Eq.(2) results in overestimating η, and underestimating ν_p and k_p [21–23]. The results are reported in Fig. 4, where for both the represented quantities k_p and η, the same criteria "the higher the better" holds in the perspective of losses reduction. From Fig. 4 one sees that YBCO (with artificial pinning centers) is favoured with respect to Nb_3Sn both in higher pinning and for lower dissipation (higher η). The field dependences bring interesting information: k_p in YBCO is essentially constant, an indication of a single-vortex pinning regime [24]; in Nb_3Sn, on the other hand, k_p decreases by a factor ~2. Similarly, the viscosities shows a Bardeen-Stephen [25] like behaviour in YBCO, and to a slightly lesser extent also in Nb_3Sn.

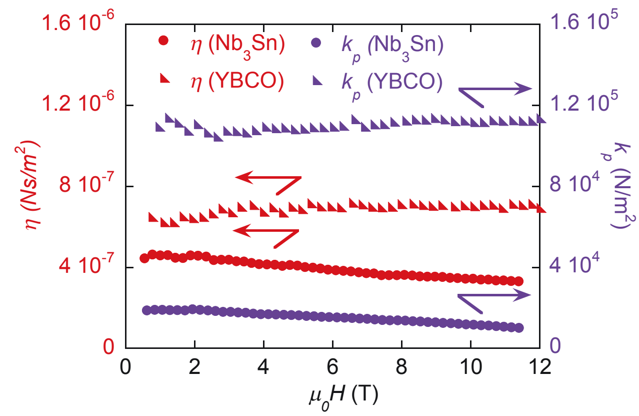

Figure 4: Fluxon parameters extracted from the vortex motion resistivity reported in Fig. 3.

The comparison of the results in Nb_3Sn and YBCO at the same reduced temperature T/T_c is instructive on different levels. The absolute values of the vortex motion resistivity clearly show the beneficial role (from the point of view of the reduced dissipation) of engineered defects in YBCO. Since this path has not been explored previously in Nb_3Sn, it cannot be excluded that novel routes toward the introduction of effective pinning centers could bring forward Nb_3Sn even for rf/microwave applications in high magnetic fields. This is reinforced by the analysis of the pinning constant, which shows that in YBCO with $BaZrO_3$ second phase nanoparticles the vortices are individually pinned, while at the same vortex density this is not the case in Nb_3Sn.

A less positive message comes from the vortex viscosity: at the same reduced temperature and flux density it seems that the intrinsic losses in Nb_3Sn are larger than in YBCO (more likely, due to the lower upper critical field in Nb_3Sn), which implies (cfr. Fig. 1) a larger dissipation. This impact both the choice of superconducting materials, and also the strategy of the eventual pinning optimization approach, depending on the specific application since the potential impact of the added defects on η must be kept in consideration. Indeed, a correlation between η and k_p can be expected, as the one observed in Nb rf cavities when considering the residual resistance due to trapped fluxons, interpreted in terms of the common dependence on the electron mean free path [26]. Thus, novel strategies for material optimization must be conceived.

CONCLUSIONS

We have presented high magnetic field (≤ 12 T) measurements of the surface impedance of technological relevant superconductors, Nb_3Sn and $YBa_2Cu_3O_{7-\delta}$, in bulk and thin film form, respectively, performed at 14.9 GHz. By analysing the data through high frequency models for the vortex motion resistivity, a normalized (irrespective to the sample geometry) comparison of the vortex motion induced losses has been proposed, highlighting the better behaviour of YBCO. Moreover, the relevant vortex parameters have been extracted, which allows to ascertain the roles played by the various vortex motion mechanisms (and corresponding "lumped" parameters). In particular, it has been shown that vortex pinning is important to limit losses, but cannot be the sole focus of a material optimization process since the flux flow resistivity brings an important contribution.

ACKNOWLEDGEMENTS

This work has been partially carried out within the framework of the EUROfusion consortium, Agency funding from the Euratom research and training programme 2014-18 and 2019-20 under grant agreement No. 633053, and partially supported by the FCC collaboration under MoU Addendum FCC-GOV-CC-0218 (KE5084/ATS) between CERN and the Department of Engineering, University Roma Tre.

REFERENCES

[1] S. Calatroni, "HTS Coatings for Impedance Reduction in Particle Accelerators: Case Study for the FCC at CERN," *IEEE Trans. Appl. Supercond.*, vol. 26, no. 3, art. id. 3500204, Apr. 2016. doi: 10.1109/TASC.2016.2520079

[2] D. Alesini *et al.*, "Galactic axions search with a superconducting resonant cavity," *Phys. Rev. D*, vol. 99, art. id. 101101(R), Mar. 2019. doi: 10.1103/PhysRevD.99.101101

[3] J. MacManus-Driscoll *et al.*, "Strongly enhanced current densities in superconducting coated conductors of $YBa_2Cu_3O_{7-x}$ + $BaZrO_3$." *Nat. Mater.*, vol. 3, no. 7, pp. 439–443, Jul. 2004. doi: 10.1038/nmat1156

[4] B. Maiorov *et al.*, "Synergetic combination of different types of defect to optimize pinning landscape using BaZrO(3)-doped YBa(2)Cu(3)O(7)." *Nat. Mater.*, vol. 8, no. 5, pp. 398–404, May 2009. doi: 10.1038/nmat2408

[5] N. Pompeo, R. Rogai, E. Silva, A. Augieri, V. Galluzzi, and G. Celentano, "Strong reduction of field-dependent microwave surface resistance in $YBa_2Cu_3O_{7-\delta}$ with submicrometric $BaZrO_3$ inclusions," *Appl. Phys. Lett.*, vol. 91, no. 18, art. id. 182507, Oct. 2007. doi: 10.1063/1.2803856

[6] N. Pompeo, A. Augieri, K. Torokhtii, V. Galluzzi, G. Celentano, and E. Silva, "Anisotropy and directional pinning in $YBa_2Cu_3O_{7-x}$ with $BaZrO_3$ nanorods," *Appl. Phys. Lett.*, vol. 103, no. 2, art. id. 022603, Jul. 2013. doi:10.1063/1.4813405

[7] K. Torokhtii *et al.*, "Measurement of Vortex Pinning in YBCO and YBCO / BZO Coated Conductors Using a Microwave Technique," *IEEE Trans. Appl. Supercond.*, vol. 26, no. 3, art. id. 8001605, Apr. 2016. doi:10.1109/TASC.2016.2550019

[8] N. Pompeo, K. Torokhtii, and E. Silva, "Extraction of the Complex Resistivity and Pinning Parameters from Microwave Surface Impedance Measurements of Coated Conductors," *IEEE Trans. Appl. Supercond.*, vol. 28, no. 4, art. id. 9000505, Jun. 2018. doi: 10.1109/TASC.2018.2797307

[9] N. Pompeo *et al.*, "Intrinsic anisotropy and pinning anisotropy in nanostructured $YBa_2Cu_3O_{7-\delta}$ from microwave measurements," *Supercond. Sci. Technol.*, vol. 33, no. 4, art. id. 044017, Mar. 2020.

[10] A. Romanov *et al.*, "High frequency response of thick REBCO coated conductors in the framework of the FCC study," *Sci. Rep.*, vol. 10, no. 1, art. id. 12325, 2020. doi: 10.1038/s41598-020-69004-z

[11] A. Alimenti *et al.*, "Microwave surface impedance measurements in nanostructured YBCO up to high magnetic fields," presented at ASC 2020 Virtual Conf., 24 Oct.– 7 Nov., 2020, paper Wk2LOr2D–03, unpublished.

[12] J. Lee *et al.*, "Grain-boundary structure and segregation in Nb_3Sn coatings on Nb for high-performance superconducting radiofrequency cavity applications," *Acta Mater.*, vol. 188, pp. 155–165, Feb. 2020 doi:10.1016/j.actamat.2020.01.055

[13] M. W. Coffey and J. R. Clem, "Unified Theory of Effects of Vortex Pinning and Flux Creep upon the rf Surface impedance of Type-II Superconductors," *Phys. Rev. Lett.*, vol. 67, no. 3, pp. 386–389, Jul. 1991. doi: 10.1103/PhysRevLett.67.386

[14] J. I. Gittleman and B. Rosenblum, "Radio-frequency resistance in the mixed state for subcritical currents," *Phys. Rev. Lett.*, vol. 16, no. 17, pp. 734–736, Apr. 1966. doi: 10.1103/PhysRevLett.16.734

[15] A. Alimenti, K. Torokhtii, E. Silva, and N. Pompeo, "Challenging microwave resonant measurement techniques for conducting material characterization," *Meas. Sci. Technol.*, vol. 30, art. id. 065601, May 2019. doi:10.1088/1361-6501/ab0e65

[16] K. Torokhtii, A. Alimenti, N. Pompeo, and E. Silva, "Estimation of microwave resonant measurements uncertainty from uncalibrated data," in Acta IMEKO, 2020, vol. 9, no. 3, pp. 47—52.

[17] K. Torokhtii *et al.*, "Microwave Measurements of Pinning Properties in Chemically Deposited YBCO / BZO Films," *IEEE Trans. Appl. Supercond.*, vol. 27, no. 4, art. id. 8000405, Jun. 2017.

[18] T. Spina, "Proton irradiation effects on Nb_3Sn wires and thin platelets in view of High Luminosity LHC upgrade," Ph.D. thesis, University of Geneva, 2015.

[19] A. Alimenti *et al.*, "Microwave measurements of the high magnetic field vortex motion pinning parameters in Nb_3Sn," *Supercond. Sci. Technol.*, vol. 34, art. id. 014003, 2021. doi:10.1088/1361-6668/abc05d

[20] N. Pompeo, K. Torokhtii, and E. Silva, "Surface impedance measurements in thin conducting films: Substrate and finite-thickness-induced uncertainties," in *2017 IEEE Int. Instrum. Meas. Technol. Conf.*, 22-25 May 2017, pp. 1–5. doi:10.1109/I2MTC.2017.7969902

[21] N. Pompeo and E. Silva, "Reliable determination of vortex parameters from measurements of the microwave complex resistivity," *Phys. Rev. B*, vol. 78, no. 9, art. id. 094503, Sep. 2008. doi: 10.1103/PhysRevB.78.094503

[22] N. Pompeo, A. Alimenti, K. Torokhtii, G. Sylva, V. Braccini, and E. Silva, "Pinning, flux flow resistivity and anisotropy of Fe(Se,Te) thin films from microwave measurements through a bitonal dielectric resonator," *IEEE Trans. Appl. Supercond.*, vol. 31, no. 5, art. id. 8000805, Aug. 2021. doi:10.1109/TASC.2021.3063665

[23] N. Pompeo, K. Torokhtii, A. Alimenti, and E. Silva, "A method based on a dual frequency resonator to estimate physical parameters of superconductors from surface impedance measurements in a magnetic field," *submitted for publication*.

ISBN: 978-3-95450-233-2 ISSN: 2673-5504 doi:10.18429/JACoW-SRF2021-TUPFDV007

[24] M. Golosovsky, M. Tsindlekht, and D. Davidov, "High-frequency vortex dynamics in $YBa_2Cu_3O_7$," *Supercond. Sci. Technol.*, vol. 9, no. 1, pp. 1–15, 1996. doi: 10.1088/0953-2048/9/1/001

[25] J. Bardeen and M. Stephen, "Theory of the Motion of Vortices in Superconductors," *Phys. Rev.*, vol. 140, no. 4A, pp. 1197–1207, Nov. 1965. doi: 10.1103/PhysRev.140.A1197

[26] M. Checchin, M. Martinello, A. Grassellino, A. Romanenko, and J. F. Zasadzinski, "Electron mean free path dependence of the vortex surface impedance," *Supercond. Sci. Technol.*, vol. 30, no. 3, art. id. 034003, Jan. 2017. doi:10.1088/1361-6668/aa5297